"Fatigue Anisotropy in a Wrought Aluminum Alloy"

A. Zabett and A. Plumtree

Presented to:

The Fifth International Conference on Fatigue and Fatigue Thresholds;

held 3-7 may 1993, Montreal, Quebec, Canada.

Fatigue 93, Edited by J.P. Bailon and J.I. Dickson, Volume 1, pp. 421-426.

FATIGUE ANISOTROPY IN A WROUGHT ALUMINUM ALLOY

A. ZABETT* and A. PLUMTREE*

The influence of anisotropic microstructure on fatigue crack nucleation and short crack growth of a wrought aluminum alloy was studied at an intermediate stress amplitude. The longitudinal direction specimens had the shortest lives caused by early nucleation of cracks from particles. The transverse direction specimens possessed the longest lives since more grain boundaries hindered fatigue crack growth.

INTRODUCTION

The deformation required to produce a wrought alloy usually results in mechanical fibering and anisotropic properties. In materials with an anisotropic microstructure, varying the grain boundary spacing and possible directionality as well as arrangement of second phase particles in different orientations cause different mechanical behaviour. Although the influence of grain boundaries and second phase particles on short fatigue crack growth has been studied[1], the influence of variations in grain dimensions within the same material is not well documented. Consequently, the objective of this work is to study those effects on the fatigue life and short crack behaviour of one material, namely 2024-T351 aluminum alloy.

EXPERIMENTAL PROCEDURE

Round smooth fatigue test specimens were machined from a slab of rolled aluminum alloy, 2024-T351 for three different orientations namely longitudinal (L-direction), transverse (T-direction), and short transverse (S-direction). The specimens with a gauge length of 10.16 mm and diameter of 6.35 mm were polished with emery paper to 600 grit and then diamond paste of 1 μm and 1/4

* Department of Mechanical Engineering, University of Waterloo, Canada

TABLE 1 - Tensile Strength and Fatigue Lives.

Orientation	σ_{TS} MPa/ksi	σ_a MPa/ksi	Number of Tests	Average life (Cycles)	Population Standard Deviation
L-direction	478/69.4	214/31.1	5	127040	36421
S-direction	431/62.5	193/28.0	5	142640	26235
T-direction	466/67.6	208/30.2	6	235700	76995

μm. Grain orientations were determined by examining one end of each specimen after etching. All tests were carried out on a servo-controlled electrohydraulic testing machine at a stress ratio of R=-1 and frequency of 25 Hz. A normalized stress amplitude of σ_a/σ_{TS} of 0.45 was applied for all tests, see Table 1. A replicating technique using acetate tape was employed to study the number and growth of surface cracks.

RESULTS AND DISCUSSION

The fatigue life results are summarized in Table 1. The T-direction specimens possessed the longest average life of 235,700 cycles. The L-direction gave the shortest average life of 127,040 cycles and the S-direction had an intermediate average life of 142,640 cycles.

Crack growth studies of all three orientations showed differences in short fatigue crack behaviour. Fig. 1 shows that the growth of a surface crack to 1000 μm was fastest in the L-direction.

The number of surface cracks on each specimen was considered by counting cracks using replicas taken from the gauge length after cycling the specimens at a normalized stress amplitude σ_a/σ_{TS} of 0.45 for 100,000 cycles. The average number of cracks longer than 100 μm in the L-direction specimens was more than 100. For the S- and T-directions the numbers were much lower and were 10-20 and 1-5 respectively.

Careful examination of the surfaces of L-direction specimens during and after testing revealed that almost all the cracks initiated at Al_7Cu_2Fe second phase particles as indicated in Fig 2. This behaviour continued over the entire life of the specimens, leading to multiple cracking. The large number of cracks around the circumference facilitated coalescence. Consequently, the larger cracks grew faster leading to the relatively short life for the L-direction specimens, as seen in Fig 1.

Considering growth rates, the short crack behaviour varied with orientation. In general, retardation occurred at grain boundaries but very few or

TABLE 2 - Total number and location of cracks on fracture surface.

Orientation	T-dir.	S-dir.*
Number of cracks in large grains (A in Fig 1)	10	3
Number of cracks within 10°-25° of A	5	4
Number of cracks within 40°-55° of A	3	4
Number of cracks within 65°-28° of A	2	6
Number of cracks in small grains (90° to A)	2	1

* In two specimens there were many cracks all around the specimens which are not included in this table.

no stops were observed in the L-direction specimens, as seen in Fig 3. For clarity the T-direction is not included since it showed similar fatigue growth retardation at surface grain boundaries to the S-direction.

In Fig. 1 a schematic three dimensional view of the T- and S-direction specimens is included. Both orientations contained grains of 350 μm in length at the circumference. However, at 90 degrees the T-direction had grains of 38 μm while the S-direction possessed grains of 110 μm in circumferential length. The height of grains on the specimen gauge length was 110 μm for the T-direction and 38 μm for the S-direction. By contrast, in cross section, long narrow and pancake shaped grains were observed for the T- and S-directions, respectively.

Generally, cracks started within the large grains on the surface of specimens taken from these orientations (T and S). However, the number and the locations of initial cracks were different. Table 2 contains information regarding the location of initial cracks on the final fracture surface of the T- and S-direction specimens. In the S-direction specimens no preferred crack initiation sites were observed. The T-direction showed a tendency for crack nucleation to occur in those grains which had the largest circumferential length (i.e. 350 μm).

Since these large surface grains have the least constraint, thereby allowing slip to occur more easily, they are favourable locations for microcrack formation. It must be mentioned that the smaller grains on the surfaces of the S-direction specimens were still big enough to be potential sites for crack initiation, Yet the number of cracks observed in the larger surface grains (350 μm in length) was more than that in the smaller ones (110 μm in length).

The difference between the number of cracks observed on each specimen for the T- and S-orientations was related to the number of favourably oriented large grains on the surface. The number of large grains (including 110 μm grains) on the S-direction specimen surface was at least 8-9 times that in the T-direction.

It is not surprising that the number of cracks observed on the T-direction specimen surface was one or two (except for one specimen which had 5 cracks), whereas 10-20 surface cracks were counted on the S-direction specimen.

The overall crack propagation rate in the S-direction was higher than that in the T-direction. Although cracks in the T-direction were initiated at large surface grains, these grains had a depth of only 38 μm. Hence, the first barrier would be encountered at this depth. In the S-direction, surface cracks which started within either the larger (350 μm surface length) or the smaller grains (130 μm surface length), would propagate to a depth of either 110 μm or 350 μm before encountering the first grain boundary. The number of impediments to the crack tip in the T-direction was then at least 3 times that in the S-direction, resulting in a lower average crack propagation rate for the T-direction.

This is in agreement with the strain redistribution model proposed by Abdel-Raouf *et al.* [2]. Due to increasing constraint the local strain $\Delta\epsilon$ decays with depth from the surface eventually reaching the nominal strain Δe at a depth of about five grain diameters. A material with a large grain size will have a smaller rate of decay of the strain concentration factor Q_ϵ ($=\Delta\epsilon/\Delta e$) and a greater local resolved shear strain at a given depth when compared to a fine grained material. The rate of strain decay is inversely proportional to the grain size D[3] and the strain concentration factor satisfying both surface and interior conditions may be expressed by :

$$Q_\epsilon = \frac{\Delta \epsilon}{\Delta e} = 1 + q \exp\left(-\frac{a}{D}\right) \qquad (1)$$

where q is a constant. The strain concentration factor at the free surface, $Q_{\epsilon S}$, has a value of 6.3 for the grain most favourably oriented for slip[3]. As the crack length increases Q_ϵ decreases until it approaches unity. In the T-direction Q_ϵ has a higher gradient and a smaller local resolved shear strain at a given depth when compared to the S-direction. For instance, at a depth of 38 μm (equivalent to the short dimension of the first grain boundary) Q_ϵ would have a value of only 2.95 in the large T-direction surface grains, while its value would be between 4.75 (crack at A, Fig 1) and 5.75 (crack 90° from A, Fig 1) in the S-direction.

CONCLUSIONS

1. At an intermediate stress amplitude level the fatigue lives for the three orientations were in the ascending order of L-, S- and T-direction.
2. Particle cracking was found to occur early in the life of the L-direction specimen, resulting in the shortest life.
3. In the T- and S-direction specimens crack nucleation occurred most often in the larger surface grains. This caused a greater number of cracks to form in the S-direction specimens which had more large surface grains.

4. Finer grain boundary spacing in the T-direction specimens produced a greater retardation in the crack growth rate compared to the S-direction specimens. This, together with a larger number of initial cracks resulted in a shorter fatigue life of the S-direction specimens.

REFERENCES

(1) Plumtree, A. and O'Connor, B.P.D., Fatigue Fract. Engng. Mater. Struct. Vol. 14, 1991, pp. 171-184

(2) Abdel-Raouf, H., Topper, T.H. and Plumtree, A., Fatigue Fract. Engng. Mater. Struct., Vol. 15, 1992, pp. 895-909.

(3) Abdel-Raouf, H., Topper, T.H. and Plumtree, A., Scripta Metallurgica et Materialia, Vol.25, 1991, pp. 597-602.

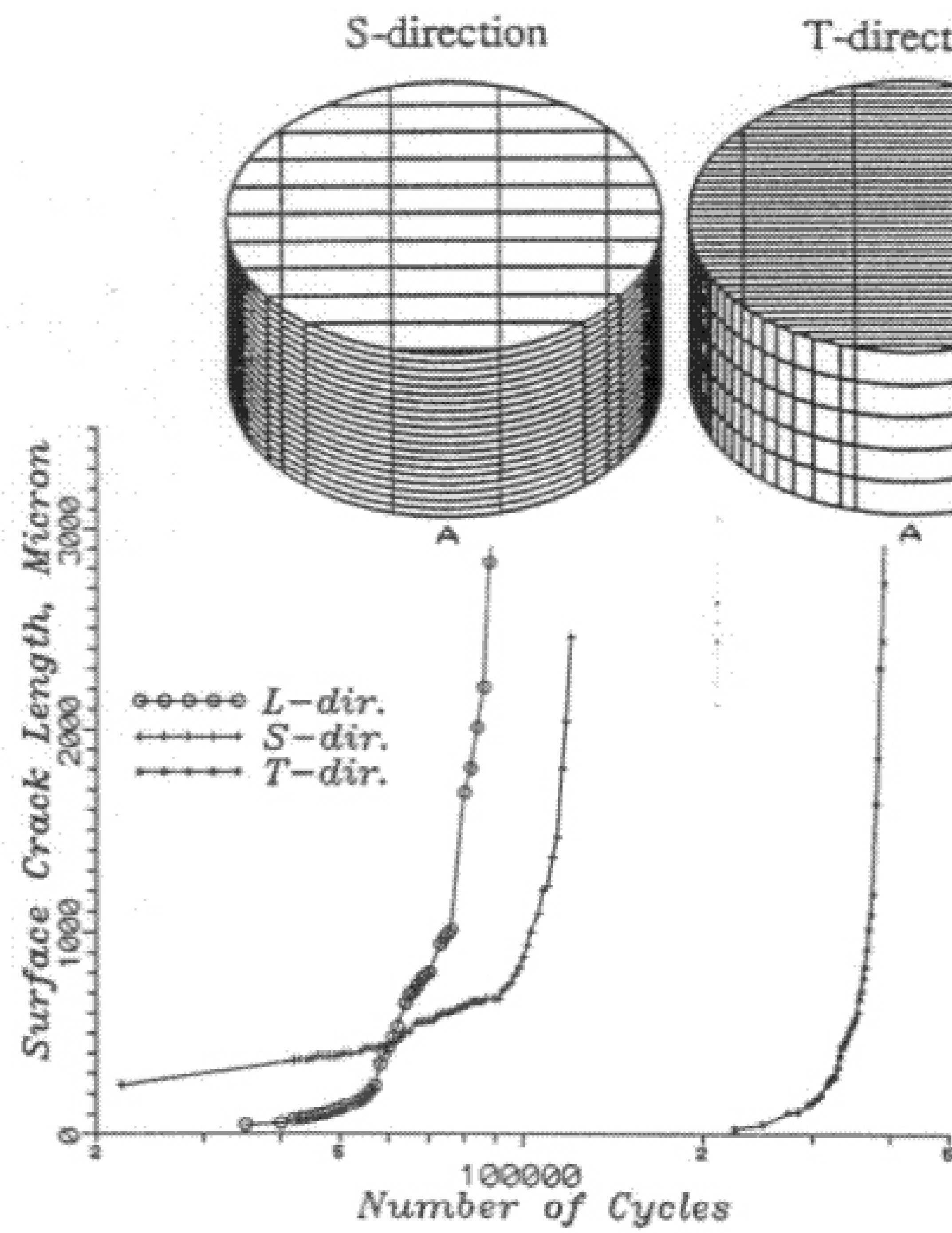

Figure 1. Representative crack growth in all three directions.

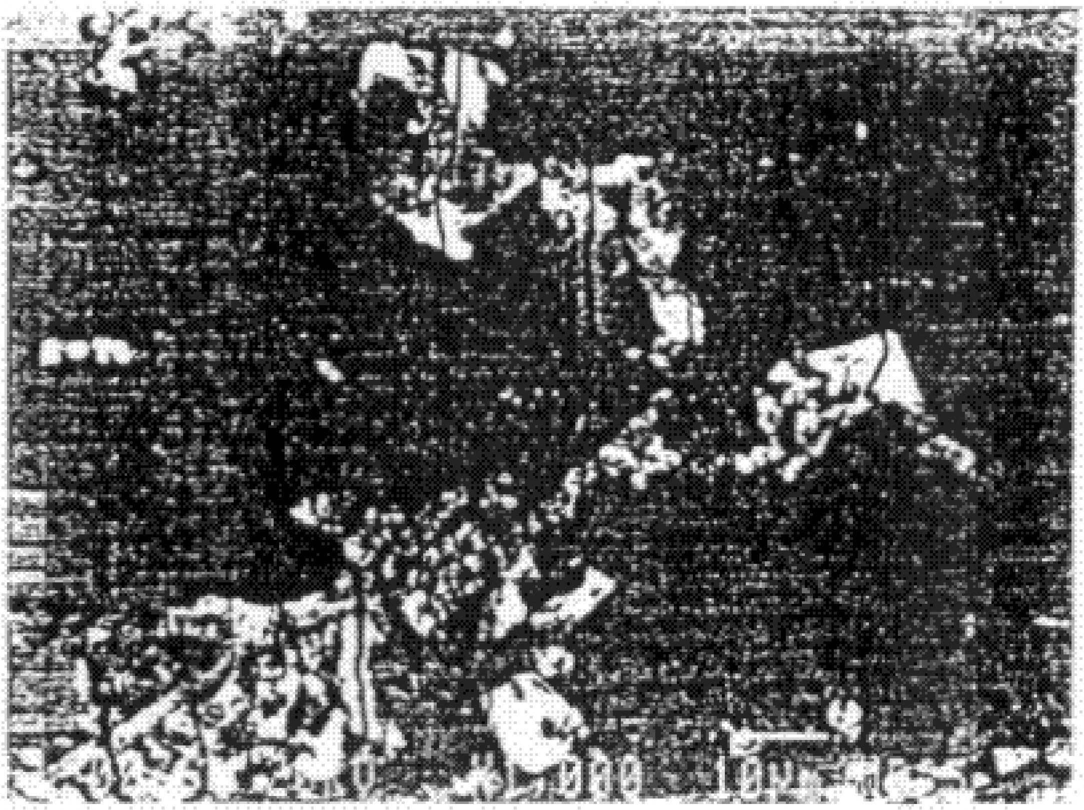

Figure 2. Particle cracking on surface of L-direction specimen. Stress axis horizontal.

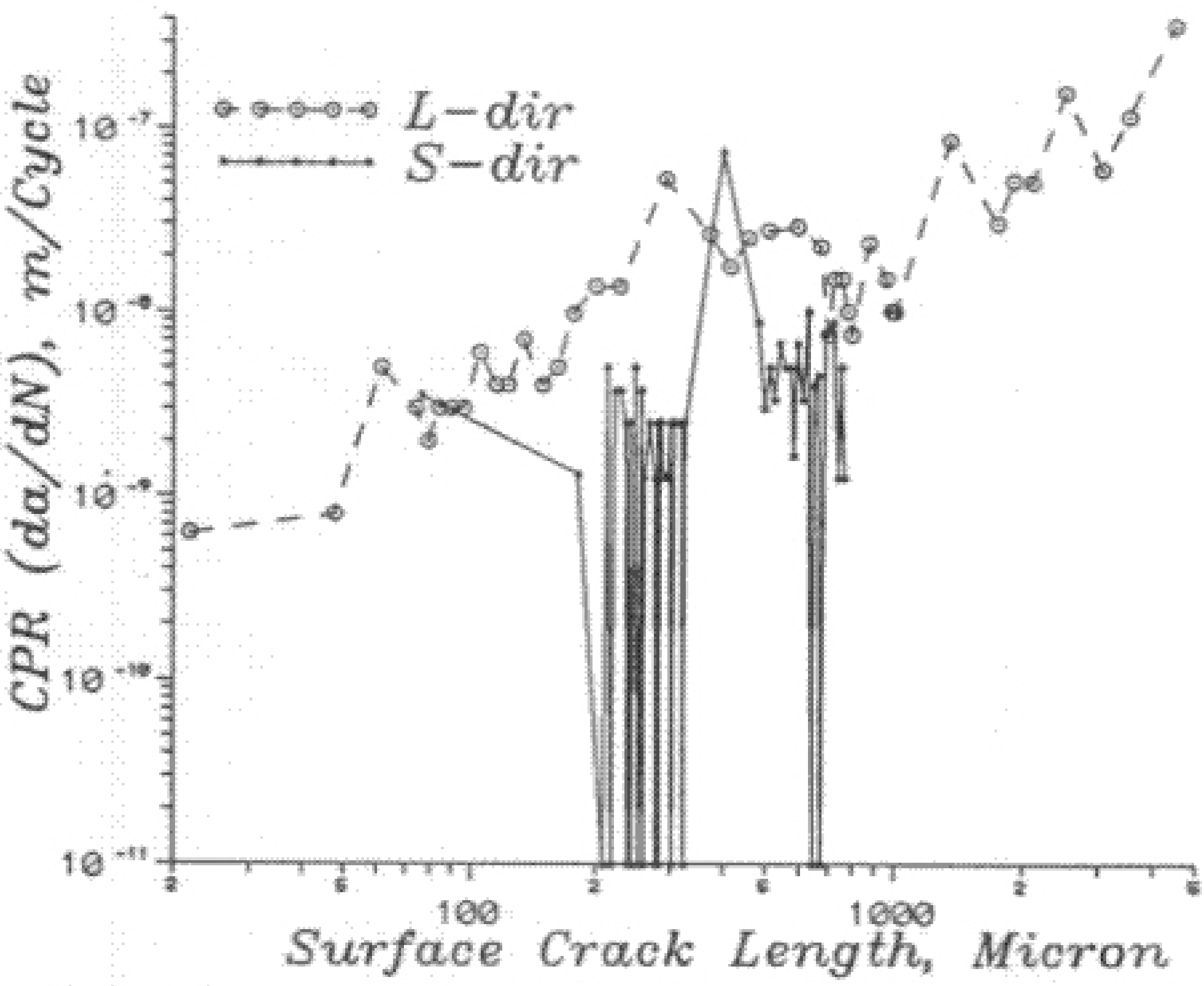

Figure 3. Typical crack growth rate for the L- and S-directions.